Desalination and Water Treatment
www.deswater.com

doi: 10.5004/dwt.2022.28480

259 (2022) 170–185
May

Comparative investigation of monomeric and micellar adsorption of cetyltrimethylammonium bromide and tetradecyltrimethylammonium bromide from their aqueous solutions

Özkan Açışlı[a], Semra Karaca[a,*], Ahmet Gürses[b]

[a]*Department of Chemistry, Faculty of Science, Atatürk University, 25240 Erzurum, Turkey, Tel. +90 442 2314435; Fax: +90 442 2360948; email: skaraca@atauni.edu.tr/semra_karaca@yahoo.com (S. Karaca), ozkan.acisli@atauni.edu.tr (Ö. Açışlı)*
[b]*Department of Chemistry, K.K. Education Faculty, Atatürk University, 25240 Erzurum, Turkey, email: agurses@atauni.edu.tr/ahmetgu@yahoo.com*

Received 25 November 2021; Accepted 5 April 2022

ABSTRACT

In this study, monomeric and micellar adsorption of cetyltrimethylammonium bromide (CTAB) and tetradecyltrimethylammonium bromide (TTAB) quaternary ammonium salts were investigated. Parameters that influence the monomeric adsorption process such as pH, adsorbent dosage, contact time, monomeric surfactant concentration and temperature were systematically studied. It was seen that these parameters have been affected the adsorption capacity of clay for CTAB and TTAB. The fit of the adsorption data to the Langmuir, Freundlich, Dubinin–Radushkevich and Temkin isotherm models was also examined. The results reveal that the Langmuir isotherm model was more suitable the equilibrium of adsorption on the clay surface. The monolayer adsorption capacities for both adsorbate were found to be 312.50 and 285.71 mg/g, respectively. Thermodynamic parameters showed that the adsorption process was spontaneous and exothermic. Adsorption enthalpy and entropy changes for both adsorbates were calculated as –10.6 and –6.6 kJ/mol and 18.0 and 14.9 J/mol K, respectively. The kinetic results can be represented by pseudo-second-order model implying the stronger interactions between clay surface and surfactant ions. The variation of the micellar adsorption capacity with temperature and initial surfactant concentration revealed the changing in micellar forms. The different behaviors of CTAB and TTAB, which may occur depending on the temperature, show that the chain transfer energy, which varies with the tail length, has a dominant effect on the micellar adsorption.

Keywords: Adsorption; Surfactant; Cetyltrimethylammonium bromide, Tetradecyltrimethylammonium bromide; Enthalpy of adsorption, Adsorption isotherm, Adsorption kinetics

1. Introduction

Surfactant molecules having a hydrophilic head and a hydrophobic tail group are formed micelles, which consist of an ionic surface and a hydrophobic core, after reaching a certain concentration value in the aqueous solution. Micelles are generally defined as core-shell surfactant systems dispersed in the bulk phase [1]. The head parts of the surfactant molecules are located on the micelle surface and form an electrical double layer around the micelle surface [2–4]. The size and shape of the micelles are significantly influenced by the type of surface active material as well as solution conditions, including ionic strength, pH, surfactant concentration and temperature [5]. Surfactants, which have detergent, wetting, emulsifying, solvent, dispersant and foaming properties, are also used in many fields, including cosmetics [6]. Micelles,

* Corresponding author.

which are self-assembled aggregates, are widely used in many different fields such as preparation of photofunctional dyes and sensors, targeted drug delivery, pharmacology, medicine and cosmetics [7,8].

The decrease in the surface tension with the adsorption and micellization of surfactant molecules in solutions is great of importance for the numerous applications such as the stability control, transport for crude oil, flotation and rheology for dispersed systems in different technological processes [7,9–11]. Surfactants play a key role in adsorption at the interface and aggregation in bulk solution. Therefore, an understanding of the physicochemical properties of surfactants at the surface is crucial in determining the best practice to use. Cationic surfactants form a strong adsorption layer on negatively charged surfaces [9]. In general, surfactant adsorption onto solid/water interfaces occurs via covalent bonding, electrostatic attraction, hydrogen bonding, solvation, desolvation, lateral associative interaction, or non-polar interactions between the adsorbed particles. Total adsorption usually takes place over some or all of the above forces [12,13].

Montmorillonite, a natural clay mineral class, is widely used in many areas and especially in environmental remediation activities due to its superior properties such as excellent swelling ability, high cation exchange capacity (CEC), large specific surface area, high charge density, abundance and cheapness [14,15].

In addition, by adsorption of cationic surfactants on the montmorillonite surface, hydrophobic organo-clays with zero or positive net surface charge and increased basal distance between layers can be obtained [12,16,17].

Therefore, understanding surfactant adsorption mechanisms in terms of the various forces involved and the factors that control them is of great importance [12]. The technological application of surfactant systems in industrial fields requires detailed knowledge of various physicochemical properties such as size, geometry, packing density, conductivity and the type of interactions between surfactant-adsorbent [5,13]. For this reason, the present study is devoted to the investigation of monomeric and micellar adsorption on the montmorillonite surface from aqueous solutions of two cationic surfactants, such as cetyltrimethylammonium bromide (CTAB) and tetradecyltrimethylammonium bromide (TTAB), with different chain lengths and conformations. The effect of some parameters such as initial surfactant concentration, initial solution pH, adsorption temperature, adsorbent dosage and adsorption time on the process were investigated and compared with each other. The adsorption data were supported by the measurements of zeta potential of solid particles in suspensions and electrical conductivity. The obtained data were also applied to adsorption kinetic and equilibrium isotherm models, and thermodynamic quantities such as adsorption Gibbs free energy change and adsorption enthalpy and entropy changes were calculated. Finally, the micellization behavior of CTAB and TTAB was investigated as a function of surfactant concentration and temperature. In addition, these results were evaluated in terms of changes in the surface topography by taking High-resolution scanning electron microscope (HR-SEM) images.

2. Material and methods

2.1. Material

Montmorillonite, which is a commercial sample of bentonite from Çankırı deposit in Turkey, was supplied from Karakaya Mineral Co., Ankara, Turkey to use as adsorbent. The cation exchange capacity (CEC) of the clay sample was found to be 149 meq/100 g by the methylene blue method [18]. The specific surface area of bentonite clay, Brunauer–Emmett–Teller (N_2), was measured as 69.4 m^2/g. Chemical composition (wt.%) of the clay determined by X-ray fluorescence spectrometer are: SiO_2 (59.320), Al_2O_3 (17.190), Fe_2O_3 (5.949), MgO (3.632), CaO (2.211), Na_2O (1.667), K_2O (0.097), TiO_2 (0.743), SO_3 (0.506) and others (7.807). Cetyltrimethylammonium bromide (CTAB), tetradecyltrimethylammonium bromide (TTAB) and other materials were bought from Sigma-Aldrich Co., (USA). The specifications of CTAB and TTAB are given in Table 1. All chemicals were of analytical grade and were used without any further purification. Distilled water was used throughout the experiments.

2.2. Adsorption experiments

Batch adsorption experiments were performed in 100 mL glass-stoppered round-bottom flasks in a temperature-controlled thermostatic shaker (Julabo SW22, Germany) which can be controlled its temperature, time and stirring speed. In each run, 100 mL of the CTAB and TTAB solutions with known concentration and certain dosage of clay were used and adsorption experiments was carried out for certain times at the temperatures of 293, 313 and 323 K and at constant stirring speed of 150 min^{-1}. The effect of clay dosage (0.8–2.5 g/L), concentration of CTAB (50–300 mg/L for monomeric adsorption, 330–410 mg/L for micellar adsorption), concentration of TTAB (200–1,000 mg/L for monomeric adsorption, 1,110–1,200 mg/L for micellar adsorption), pH (1.0–11.0), adsorption time (5–60 min) on surfactant removal were investigated. The initial solution pH was adjusted with NaOH or HCl (0.1 M) and measured using a Mettler Toledo pH meter (China), which was standardized with buffers before every measurement. At the end of each adsorption run, the treated solution was centrifuged for 5 min at 6,000 min^{-1} (Hettich EBA 20, Germany). Then, the surfactant concentration in the supernatant was determined using the Varian Cary 100 UV-Vis spectrophotometer (Australia) at a maximum wavelength of 375 nm. Measurements were made in the presence of 0.02 mL of 0.1% picric acid and 0.40 mL of 1, 2-dichloroethane per 1.0 mL of supernatant. Surfactant-free blanks were used for each set of experiments. The amount of surfactant adsorbed per gram of adsorbent was calculated using the following equation:

$$q = \frac{(C_0 - C_e)V}{m} \tag{1}$$

where q is the amount surfactant adsorbed per gram of adsorbent (mg/g), C_0 and C_e are the initial and the equilibrium surfactant concentrations (mg/L) respectively. V is the

Table 1
The main characteristics of surfactants used in this study

Chemical name	Molecular structure	Molar mass (g/mol)	CMC (mol/L)	CAS No
Cetyltrimethylammonium bromide, (CTAB) $CH_3(CH_2)_{15}N(Br)(CH_3)_3$	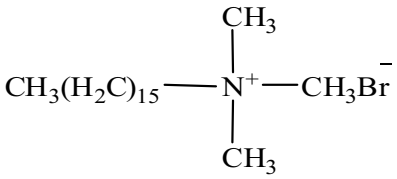	364.45	9.01×10^{-4}	57-09-0
Tetradecyltrimethylammonium bromide, (TTAB) $CH_3(CH_2)_{13}N(Br)(CH_3)_3$	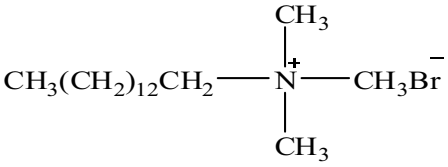	336.39	3.3×10^{-3}	1119-97-7

volume of solution (L), and m is the dry weight of added adsorbent (g).

2.3. Zeta potential and conductivity measurements

Zeta potentials of solid particles in organoclay/water suspensions from the experiments at various pH values were measured using Zeta-Meter 3.0+ (Zeta-Meter, Inc., Staunton, VA, USA) for a constant adsorption time, 30 min. In the experiments initial surfactant concentrations were 300 mg/L and clay concentration 1.0 g/L and 1.5 g for CTAB and TTAB, respectively. The zeta potential values were corrected for temperature differences using the following equation:

$$\xi_d\left(\mathrm{mV}\right) = C_T\xi_0 \tag{2}$$

where ξ_d, C_T, ξ_0 represent the corrected zeta potential value, correction factor related to temperature and the measured zeta potential value, respectively. In addition, before each measurement, the zeta meter was calibrated using a Min-U-Sil standard solution. Also, conductivity measurements were made after adsorption used the WTW LF 521 Karl Kolb conductometer (WTW Inc., Weilheim, Germany) under the same conditions as the zeta potential measurements.

2.4. Characterization of the samples

The crystal structure of the Çankırı clay was characterized by X-ray diffraction analysis (Panalytical Empyrean diffractometer with Cu-Kα radiation (40 kV, 15 mA, 1.54051 Å)) at room temperature, and the scan range was set from 5° to 70°. The images of high-resolution scanning electron microscope (HR-SEM) were recorded by a Zeiss Sigma 300 SEM instrument equipped with EDAX analyzer (Zeiss, Germany).

2.5. Equilibrium isotherms

Equilibrium adsorption isotherms, which are extremely important in the design of adsorption systems and explain the interaction mechanism between adsorbent and adsorbate at equilibrium, have also been investigated [16,18]. The equilibrium adsorption data obtained for 30 min were applied to the isotherm equations by using SPSS 24.0 package program. In this analysis the linear forms of isotherm equations (Table 2) were used to determine the fitting of the adsorption of two quaternary ammonium salts (CTAB and TTAB) on montmorillonite to isotherm models such as Langmuir, Freundlich, Temkin and Dubinin–Radushkevich.

2.6. Thermodynamic investigations

The calculation of thermodynamic parameters is very important to determine the feasibility and spontaneity of the adsorption process as well as the effect of temperature. For this, adsorption enthalpy and entropy changes were calculated using Eq. (3). It was assumed that the enthalpy and the entropy changes in the operating temperature range are independent of temperature [15,19].

$$\ln K_{\mathrm{eq}} = -\frac{\Delta H^{\circ}_{\mathrm{ads}}}{RT} + \frac{\Delta S^{\circ}_{\mathrm{ads}}}{R} \tag{3}$$

$$\Delta G^{\circ}_{\mathrm{ads}} = -RT\ln K_{\mathrm{eq}} \tag{4}$$

where T and R represent the absolute temperature and gas constant, respectively.

In this equations, the Langmuir isotherm constant, K_{eq} was used instead of the equilibrium constant by various changes to become dimensionless [20,21].

2.7. Adsorption kinetics

A simple kinetic analysis of adsorption is the Lagergren's pseudo-first-order equation:

$$\ln\left(q_e - q_t\right) = \ln q_e - k_1 t \tag{5}$$

where q_t is the amount of dye adsorbed at time t (mg/g), q_e is the adsorbed amount of dye at equilibrium, and k_1 is

Table 2
Equations of the isotherms used for both surfactants, CTAB and TTAB at three temperatures, and the isotherm parameters calculated for them

Isotherm equation	Temp. (K)	Constant parameters	CTAB	TTAB
Langmuir $\frac{C_e}{q_e}=\frac{1}{q_m\cdot K}+\frac{C_e}{q_m}$	293	q_m	312.5	285.71
		K	3.200	1.167
		R_L	0.510	0.575
		R^2	0.992	0.996
	313	q_m	303.0	277.78
		K	3.300	1.385
		R_L	0.503	0.575
		R^2	0.988	0.997
	323	q_m	303.0	277.8
		K	2.538	1.286
		R_L	0.568	0.638
		R^2	0.994	0.998
Freundlich $\ln q_e=\ln K_f+n\ln C_e$	293	n	0.322	0.169
		K_f	194.202	167.721
		R^2	0.988	0.950
	313	n	0.215	0.143
		K_f	194.008	174.443
		R^2	0.980	0.943
	323	n	0.312	0.143
		K_f	177.647	174.863
		R^2	0.984	0.964
Temkin $q=\left(\frac{RT}{b_T}\right)\ln a_T+\left(\frac{RT}{b_T}\right)\ln C$	293	b_T	1.243	0.938
		a_T	112.164	168.289
		R^2	0.967	0.977
	313	b_T	1.247	0.779
		a_T	28.421	463.337
		R^2	0.867	0.975
	323	b_T	1.204	0.724
		a_T	97.709	617.577
		R^2	0.972	0.984
Dubinin–Radukevisch $\ln q=K\varepsilon^2+\ln q_{DR}$	293	K	–2.00.10–8	–7.00.10–8
		q_{DR}	217.761	247.299
		E (kJ/mol)	5.00	2.67
		R^2	0.872	0.880
	313	K	–5.00.10–9	–4.00.10–8
		q_{DR}	198.721	245.574
		E (kJ/mol)	10.00	3.54
		R^2	0.772	0.880
	323	K	–2.00.10–8	–3.00.10–8
		q_{DR}	213.343	242.209
		E (kJ/mol)	5.00	4.08
		R^2	0.859	0.849

q, adsorption capacity of surfactant (mg/g); q_m, monolayer adsorption capacity; C_e, equilibrium concentration; n, K and K_f are constant parameters for the isotherm equations.

the rate constant of pseudo-first-order adsorption. The rate constant, k_1 was determined from slope of the linear plots of $\ln(q_e - q_t)$ against t.

The linear form of pseudo-second-order kinetic as follows

$$\frac{t}{q_t} = \frac{1}{k_2 q_e^2} + \frac{t}{q_e} \tag{6}$$

where k_2 is the rate constant of pseudo-second-order adsorption. The adsorbed amount of dye at equilibrium (q_e) and the rate constant (k_2) can be calculated from the intercept and slope of the plot of (t/q_t) vs. t.

The intraparticle diffusion model:

$$q_t = k_i t^{1/2} + C \tag{7}$$

where q_t is the amount of dye adsorbed at time t (mg/g), k_i is the intraparticle diffusion rate constant (mg/s$^{1/2}$ g), and C is the intercept. According to Eq. (7) a plot of q_t vs. $t^{1/2}$ should be a straight line with a slope k_i and intercept C when the adsorption mechanism follows the intraparticle diffusion process.

In order to quantitatively compare the applicability of the models, a normalized standard deviation Δq is calculated [22,23],

$$\Delta q(\%) = \sqrt{\frac{\sum\left[\frac{q_{t,\exp} - q_{t,\text{cal}}}{q_{t,\exp}}\right]^2}{(n-1)}} \cdot 100 \tag{8}$$

where n is the number of data points, $q_{t,\exp}$ is the experimental adsorption capacity and $q_{t,\text{cal}}$ is the calculated adsorption capacity.

3. Results and discussion

3.1. X-ray diffraction analysis

The X-ray diffraction spectrum of crude montmorillonite (MMT) is given in Fig. 1. The peaks at 7.60°, 19.82°, 36.12°, 54.53° and 62.09° are characteristic peaks of montmorillonite clay and the peaks at 22.03° and 34.96° can be attributed to the quartz phase [24–26].

3.2. Effect of contact time and initial surfactant concentration on the monomeric adsorption

The results obtained for the variation of the monomeric adsorption of both surfactants (CTAB and TTAB) with the contact time, at a constant stirring rate of 150 min^{-1}, at natural pH (≈7.8), at 293 K and at various initial concentrations, are shown graphically in Figs. 2 and 3, respectively. As can be seen from these figures, CTAB and TTAB adsorption can reach adsorption equilibrium in about 5 min. The extremely short equilibrium adsorption time may indicate that physical interactions are dominant in adsorption. The adsorption efficiencies of CTAB and TTAB increase with the increase in the initial surfactant concentration. The increase in the adsorption efficiency can be explained by the increase in the surfactant concentration difference between the bulk and the clay surface and thus easier diffusion [27].

Equilibrium adsorption isotherms, which are critical for the design and mechanism of the adsorption process, have also been obtained [28,29]. For this, at various initial concentrations of CTAB (50, 100,150, 200, 250 and 300 mg/L) and TTAB (200, 300, 350, 400, 450, 500, 600, 800 and 1,000 mg/L) for 30 min and at a constant mixing speed of 150 min^{-1}, at three different temperatures, experiments were carried out. The results are shown in Figs. 4 and 5. As can be seen from these figures, the isotherms obtained for both surfactants are compatible with the Type II isotherm at all temperatures. This indicates the existence of strong interactions between adsorbent and adsorbate, the heteroporous structure of the adsorbent, and cooperative adsorption at higher equilibrium concentrations [13]. With the increase of the equilibrium CTAB concentration, the adsorption efficiency and effectiveness also increase sharply (Fig. 4).

The similarity of isotherms at three different temperatures at low equilibrium concentrations may imply that the interactions occur predominantly by electrostatic interactions between CTA^+ ions and the surface SiO- groups of MMT, and in part by an ion exchange mechanism. As the concentration increases, cooperative adsorption based on the lateral interactions between the tails of the surface-bound CTAB molecules becomes effective, so the adsorption efficiency can increase significantly [12,13,30]. Fig. 4 shows that the CTAB adsorption capacity decreases with increasing temperature; the decrease is particularly evident at high equilibrium concentrations. The decrease observed in adsorption capacity with increasing temperature can be generally associated with the exothermic nature of the adsorption process [13]. The increase in temperature leads to an increase in the mobility of ions in the diffuse part of the electrical double layer around the negatively charged MMT particles. Thus, the electrical double layer expands and the thermal mobility of each clay particle increases. This may lead to a reduction in the tendency of CTAB molecules to reach the solid surface from the bulk phase [13,31]. The decrease in adsorption efficiency with increasing temperature at higher equilibrium concentrations may be attributed to the tendency of CTAB molecules to form aggregates in the bulk phase, by interaction of their tails, rather than binding to the surface. On the other hand, it can be argued that hydrophobic interactions occur only between the tails of adsorbed CTA^+ ions, with an increase in equilibrium concentration at higher temperatures [13].

It can be seen from Fig. 5 that at low equilibrium concentrations, the high adsorption efficiency and effectiveness observed by rapid binding of TTA^+ ions to the surface by electrostatic interactions do not change significantly over a wide range of equilibrium concentrations, forming a plateau. The plateau formation can be attributed to the fact that the concentration gradient between the bulk phase and the solid phase does not have a stimulating effect for adsorption, and it is likely that the change in the adsorption mechanism of TTAB to the MMT surface begins in the plateau region. In other words, as the concentration increases, hydrophobic interactions between the tails of TTA^+ ions horizontally located in the interlayer regions of the MMT

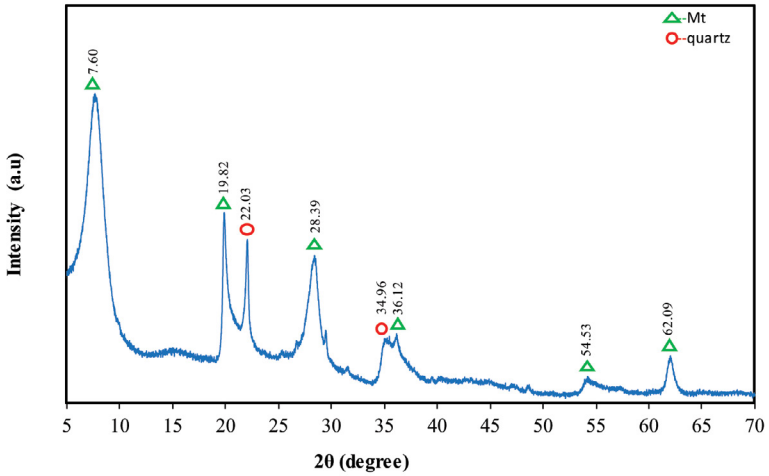

Fig. 1. X-ray diffraction pattern for the clay sample.

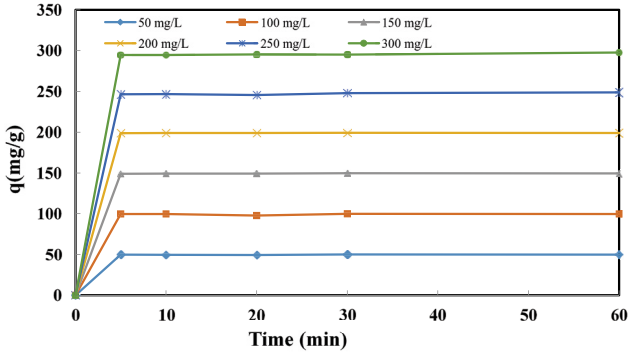

Fig. 2. Effect of initial surfactant concentration and contact time on the adsorption of CTAB onto montmorillonite (stirring speed = 150 min^{-1}; $[MMT]_0$ = 1.0 g/L; temperature = 293 K; natural pH(≈7.8)).

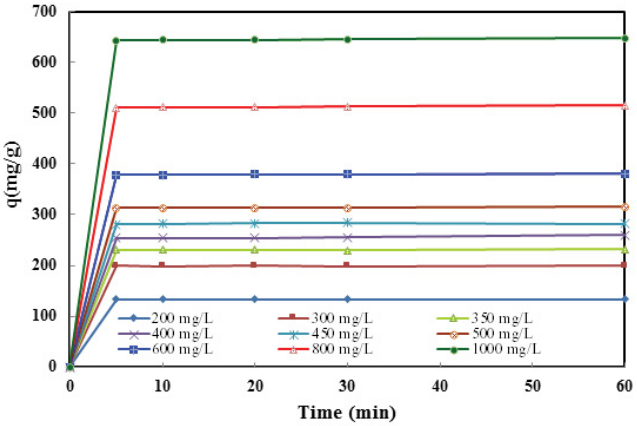

Fig. 3. Effect of initial surfactant concentration and contact time on the adsorption of TTAB onto montmorillonite (stirring speed = 150 min^{-1}; $[MMT]_0$ = 1.5 g/L; temperature = 293 K; natural pH(≈7.8)).

dominate, which can result in smaller interfacial energy and greater ionic strength. Consequently, the migration tendency of the TTA^+ ions from the bulk phase to the solid/liquid interface increase [13,31]. Therefore, the adsorption efficiency increases at higher TTAB equilibrium concentrations. The increase in temperature caused a negligible decrease in the adsorption efficiency of TTAB at low and medium equilibrium concentrations, while the decrease in efficiency was slightly greater at high equilibrium concentrations, implying the exothermic nature of adsorption.

3.3. Isotherm models and adsorption thermodynamic

In order to determine the fitting of the adsorption of two different quaternary ammonium salts of CTAB and TTAB on montmorillonite to isotherm models such as Langmuir, Freundlich, Temkin and Dubinin–Radushkevich, the equilibrium adsorption data obtained for 30 min were applied to the isotherm equations. The calculated parameters for these models were presented together with isotherm equations and regression coefficients in Table 2. The Langmuir adsorption model is based on the assumptions that the adsorption of each adsorbate molecule has the same energy, that there is no interaction between adsorbate molecules adsorbed on the adsorbent surface, and that adsorption is localized [16,32]. The high correlation coefficient values given in Table 2 show that the obtained data are in good agreement with the Langmuir isotherm at all temperatures for both surfactants.

Another analysis of the Langmuir isotherm model can be made on the basis of a dimensionless equilibrium parameter, R_L which called as separation factor and it is represented through Eq.(9) [32,33].

$$R_L = \frac{1}{1 + KC_0} \tag{9}$$

where C_0 (mg/L) is the highest initial surfactant concentration.

The values of R_L at 293, 313 and 323 K for CTAB and TTAB were between 0 and 1 which means the adsorption of both surfactants onto montmorillonite surface is favorable (Table 2).

The Freundlich isotherm equation suggests that adsorption takes place at adsorption sites with different adsorption energies by interaction between adsorbed molecules [16,33]. From Table 2 it can be seen that the experimental data fit well with the Freundlich equation for both surfactants at the entire temperature studied.

Therefore, the Freundlich constants $n < 1$ and $1/n > 1$ for the two surfactants were calculated at all temperatures and the coefficient values indicates that cooperative adsorption is effective at high surfactant concentrations [34]. The compatibility of the experimental data with both Langmuir and Freundlich isotherms shows that both monolayer adsorption and multilayer adsorption are possible due to the presence of heterogeneous active sites on the adsorbent surface [35].

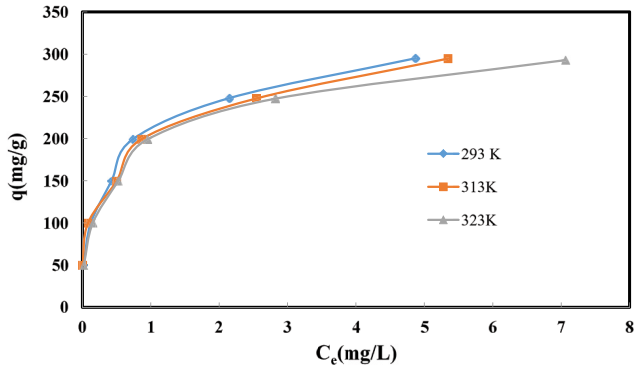

Fig. 4. Adsorption isotherms for CTAB at different temperatures (stirring speed = 150 min^{-1}; $[MMT]_0$ = 1 g/L; time: 30 min; natural pH(≈7.8)).

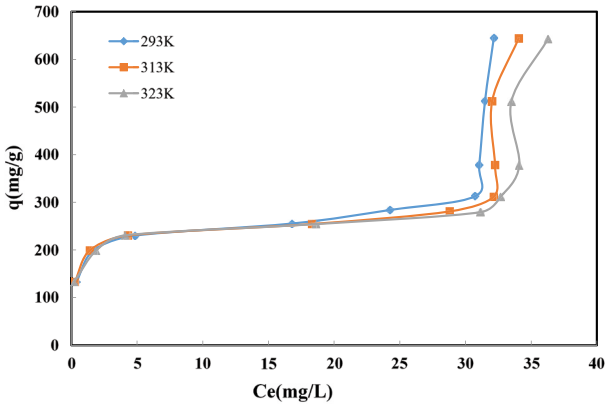

Fig. 5. Adsorption isotherms for TTAB at different temperatures (stirring speed = 150 min^{-1}; $[MMT]_0$ = 1.5 g/L; time: 30 min; natural pH(≈7.8)).

Temkin isotherm model takes into account the effects of interactions between adsorbed molecules on the adsorptive sites on the adsorption isotherms and suggest that due to these interactions the adsorption heat of all molecules in the layer decreases linearly with coverage [36,37]. The regression coefficient values given in Table 2 show that the Temkin isotherm model is in good fit with the experimental data, and even this fit increases with increasing temperature. Also, the isotherm constants were calculated and given in Table 2.This reveals that the CTAB and TTAB adsorption is characterized by a uniform distribution of binding energies up to some maximum binding energy and the increasing of temperature probably leads to increase of uniformity [16].

The fit of the equilibrium adsorption data to the Dubinin–Radushkevich isotherm model, which provides valuable information about the average energy of the molecules adsorbed per adsorbent and can be used to predict the adsorption mechanism (physical or chemical), has also been examined [27,33,38]. However, it was observed that the CTAB and TTAB adsorption were not highly fitting with this model and the fit decreased with increasing temperature (Table 2).

It is important to determine the thermodynamic parameters of an adsorption process, to find the adsorption energy, to understand whether the process is spontaneous or not, and for process design [38]. For this, for both CTAB and TTAB adsorption on the clay surface, by considering the amount of surfactant adsorbed in fixed amounts at 293, 313 and 323 K temperatures, thermodynamic quantities such as isosteric adsorption enthalpy, (ΔH°_{ads}) adsorption entropy, (ΔS°_{ads}) and the Gibbs free energy change (ΔG°) were calculated. Enthalpy and entropy changes were calculated using Eq. (3). It was assumed that the enthalpy and the entropy changes in the operating temperature range are independent of temperature [13,16]. The results obtained are listed in Table 3.

As can be seen from Table 3, negative values of enthalpy indicate that the adsorption of CTAB and TTAB is exothermic in nature, as expected. Very small enthalpy values clearly demonstrate that surfactant adsorption occurs through physical interactions, where electrostatic interaction is dominant. As is known, physical adsorption is characterized by smaller enthalpy changes (<40 kJ/mol) while chemical adsorption involves larger isosteric

Table 3
Calculated monolayer capacities and thermodynamic quantities for both surfactants, CTAB and TTAB, at three temperatures

Surfactant	T (K)	C_{eq} (mg/L)	q (mg/g)	ΔG°_{ads} (kJ/mol)	ΔH_{ads} (kJ/mol)	ΔS_{ads} (J/K mol)
CTAB (C_0: 150 mg/L)	293	0.43	149.58	–10.8	–10.6	18.0
	313	0.50	149.50	–11.2		
	323	0.52	149.48	–11.4		
TTAB (C_0: 350 mg/L)	293	4.84	230.11	–6.8	–6.6	14.9
	313	4.30	230.46	–7.1		
	323	4.08	230.61	–7.3		

adsorption heat values (>60 kJ/mol). The higher adsorption enthalpy change for CTAB can be attributed to the stronger electrostatic interactions than that of TTAB. Because the CTAB's tail volume is greater than that of TTAB and is more stringer packed. It can be said that this may be due to the closer interaction of the surfactants with the pore walls or the stronger interactions with the clay surface groups [39]. The calculated entropy value was quite lower and positive, which points to a higher affinity of clay for surfactant ions and an increased randomness at the solid–solution interface during adsorption because surfactant adsorption predominantly occurs between clay layers and partly on the surface of clay [40]. Furthermore, the exchangeable hydrated cations between the clay layers during adsorption are displaced by surfactant ions leading to an increase in entropy. Hence, it can be said that the increased entropy to be the driving force in surfactant adsorption [16,31,40].

The spontaneity of the adsorption process can be estimated by the sign and magnitude of the change in Gibbs energy $\Delta G°$ (kJ/mol) [32,38]. The calculated value from Eq. (4) is given in Table 3.

The negative values of ΔG_{ads} at all temperatures confirms the tendency for spontaneous adsorption of CTAB and TTAB on the montmorillonite surface. Interestingly, the negative value of ΔG_{ads} increased with increasing temperature.

3.4. Adsorption kinetics

Results on adsorption kinetics are important for the design of effective adsorption systems. For this reason, the obtained adsorption data were applied to three kinetic models in Eqs. (7)–(9): pseudo-first-order, pseudo-second-order and intraparticle diffusion kinetic models [27].

The parameters obtained using each of the models are shown in Table 4. From Table 4, it is evident that pseudo-second-order kinetic equation provides an excellent fit, with a linear regression coefficient $R^2 \geq 0.99$ and the theoretical $q_{e,cal}$ values agree well to the experimental $q_{e,exp}$ values at all concentrations and temperatures studied for two surfactants. So, it can be concluded that the monomeric CTAB and TTAB adsorption proceeds via a pseudo-second-order mechanism implying the stronger interactions between clay and surfactant ions. Similar results were also reported by Chowdhury et al. [27], who examined the biosorption of Basic Green 4 from aqueous solution with *Ananas comosus* (pineapple) leaf powder.

3.5. Effect of clay dosage

Experimental results on adsorbent dosage showed that the amounts adsorbed for both of surfactants is dependent on the amount of clay as shown in Figs. 6 and 7. 150 and 300 mg/L concentrations of CTAB and TTAB surfactants, respectively has been used for adsorption study at 293 K, at 150 min^{-1}, for 30 min and at natural pH. These figures show that the surfactant adsorption capacities decreased until a certain adsorbent dose and then remained constant. This constant value of adsorbent dosage was 1 g/L for CTAB and 1.5 g/L for TTAB. For this reason, these values were kept constant in the remaining experiments. As the amount of adsorbent increases, the increase in the percent removal of surfactants can be attributed to the increase in the number of active sites on the adsorbent surface. However, at higher adsorbent dosages, both difficulty in accessing the active sites of the adsorbent and an increase in diffusion path length may occur due to interactions between hydrated clay particles that prevent the diffusion of surfactant ions onto the clay surface [13,32]. This situation reveals degree of particle to particle interactions affects strongly surfactant to surface interactions.

3.6. Effect of pH

The variation of the adsorption of both surfactants with pH is shown graphically in Figs. 8–11. From Fig. 8 it can be seen that the adsorption of CTAB on clay increases in the pH 2.0–6.5 range and after a sharp increase in pH 6.5 the increase continues at a lower rate up to pH 11. On the other hand, it can be seen from this figure that the clay particles exhibit positive zeta potential values from pH 2.0 to 6.5 and negative value at pH 11.0. This change in the zeta potential values may imply that the adsorption occurs predominantly through ion exchange mechanism and partly ion pairing. The measurements of conductivity of CTAB solution at this pH range (2.0–6.5) also supports this argue (Fig. 9). The irregular change observed in conductivity in this range can also be related to the compensating of the contribution of the adsorbed CTA^+ ions to the electrical conductivity by the ions formed by the hydrolysis of some components from the adsorbent. Although the positive zeta potential value of the particles was partially decreased at pH 6.5, the amount of adsorbed may have increased due to the combination of cooperative adsorption and partially semi-micelle formation with the penetration of new ions between the CTA^+ ions adsorbed on the surface of the clay plates and intense lateral interactions. After pH 6.5, the zeta potential of the clay particles increases negatively as a result of deprotonation of the functional groups on the clay surface, but monomeric adsorption of CTA^+ ions on these sites may continue, possibly through electrostatic interactions. This is in line with the low adsorption efficiency in this region. A significant increase in conductivity after pH 6.5 can be attributed both to the presence of hydroxyl ions and to the dissolution and/or hydrolysis of some adsorbent components.

As can be seen from the experimental results of TTAB, in which the zeta potential and conductivity values and adsorption capacity changes depending on the solution pH, the zeta potential values do not show a significant change in the pH range of 2.0–3.5, but increase significantly with increasing pH (Figs. 10 and 11). Although the zeta potential values do not change in the pH 2.0–3.5 range, the increase in the adsorption capacity shows that the adsorption in this region is mainly realized by the ion exchange mechanism and after this pH value, the ion pairing adsorption mechanism becomes effective. After pH 7.0, the adsorption capacity is almost unchanged. On the other hand, the highest conductivity value at pH 2.0 decreases with increasing pH, it reaches the lowest value at pH 7.0. This demonstrates the effectiveness of the ion exchange mechanism in adsorption process at this pH range. In addition, although the adsorption capacity did not change, the increase in

Table 4
Kinetic parameters for monomeric surfactant adsorption onto montmorillonite

Surfactant	Temp. (K)	Initial concentration (mg L^{-1})	Pseudo-first-order		Pseudo-second-order			Intraparticle diffusion			
			R^2	k_2 g/mg min	$q_{e,exp}$ mg/g	$q_{e,cal}$ mg/g	Δq (%)	R^2	k_i mg/$min^{1/2}$ g	C	R^2
CTAB	293	50	0.1839	0.0112	49.6900	49.7512	0.6206	1.0000	0.6847	21.04	0.4926
	293	100	0.6539	0.0031	99.5920	100.0000	1.0214	0.9999	1.3664	42.00	0.4923
	293	150	0.0613	0.0088	149.1370	149.2537	0.2331	1.0000	2.0595	63.00	0.4949
	293	200	0.4241	0.1250	199.1140	200.0000	0.1035	1.0000	2.7414	84.12	0.4933
	293	250	0.1457	0.0007	246.7690	250.0000	1.0757	1.0000	3.4298	103.66	0.5009
	293	300	0.2151	0.0006	294.6510	294.1176	1.0255	1.0000	4.1000	124.02	0.5005
	313	50	0.2151	0.0041	48.8080	50.0000	1.3665	1.0000	0.6893	20.82	0.5009
	313	100	0.1994	0.0007	99.1140	100.0000	3.1115	0.9996	1.3741	41.06	0.5057
	313	150	0.136	0.0009	148.3920	149.2537	1.8971	0.9998	2.0480	62.10	0.4988
	313	200	0.2151	0.0077	197.3120	196.0784	0.3783	1.0000	2.7275	83.56	0.4941
	313	250	0.2151	0.0006	244.2610	250.0000	1.4528	1.0000	3.4266	102.78	0.5046
	313	300	0.3119	0.0005	292.4550	294.1176	1.6147	0.9999	4.0702	121.88	0.5054
	323	50	0.1968	0.0228	49.6450	49.7512	1.0564	1.0000	0.6915	20.72	0.5053
	323	100	0.2028	0.0041	99.0750	100.0000	0.9716	1.0000	1.3839	41.52	0.5046
	323	150	0.0107	0.001	147.0240	149.2537	1.5884	1.0000	2.0709	61.64	0.5085
	323	200	0.2422	0.0034	195.8460	196.0784	1.0920	1.0000	2.7490	82.13	0.5066
	323	250	0.2328	0.0003	240.8750	250.0000	2.9454	0.9999	3.4452	99.98	0.5211
	323	300	0.1018	0.0003	286.014	294.1176	2.3964	0.9999	4.0698	119.61	0.5161
TTAB	293	200	0.7200	0.0069	133.115	133.3333	0.0718	1.0000	1.8301	56.37	0.4915
	293	300	0.2151	0.0155	198.865	200.0000	0.0412	1.0000	2.7367	84.20	0.4920
	293	350	0.0795	0.0359	230.416	232.5581	0.6628	1.0000	3.1869	97.13	0.4967
	293	400	0.0989	0.0253	254.115	263.1579	2.4576	0.9999	3.5887	106.04	0.5122
	293	450	0.2356	0.0094	282.01	285.7143	0.4134	1.0000	3.9012	118.94	0.4966
	293	500	0.2151	0.0093	312.764	312.5000	0.8600	1.0000	4.3374	131.81	0.4982
	293	600	0.0776	0.0215	378.487	384.6154	0.6490	1.0000	5.2480	159.57	0.4979
	293	800	0.1451	0.0086	511.419	526.3158	0.7414	1.0000	7.0970	215.41	0.4988
	293	1000	0.1882	0.0053	644.110	666.6667	0.7153	1.0000	8.9304	271.08	0.4988
	313	200	0.0116	0.0511	133.128	133.3333	0.0504	1.0000	1.8326	56.33	0.4925
	313	300	0.0857	0.0057	198.513	200.0000	0.1896	1.0000	2.7376	83.99	0.4934
	313	350	0.0822	0.2054	230.296	232.5581	0.0490	1.0000	3.1721	97.40	0.4929
	313	400	0.3118	0.0013	252.606	250.0000	0.5965	1.0000	3.4886	106.74	0.4947
	313	450	0.0627	0.0007	279.344	285.7143	1.0484	1.0000	3.8996	117.52	0.5023
	313	500	0.4144	0.0028	311.971	312.5000	0.2503	1.0000	4.2896	132.26	0.4909
	313	600	0.2151	0.169	377.429	384.6154	0.1329	1.0000	5.2089	159.65	0.4939
	313	800	0.1797	0.0021	511.184	500.0000	0.2571	1.0000	7.0576	215.87	0.4949
	313	1000	0.2223	0.0012	643.486	625.0000	0.2955	1.0000	8.8841	271.53	0.4953
	323	200	0.059	0.0110	133.000	133.3333	0.1747	1.0000	1.8351	56.20	0.4943
	323	300	0.0224	0.0076	198.700	200.0000	0.1286	1.0000	2.7376	84.01	0.4933
	323	350	0.2498	0.0006	225.517	232.5581	2.1027	1.0000	3.2147	93.99	0.5174
	323	400	0.2151	0.0004	252.295	256.4103	1.8785	1.0000	3.5513	105.78	0.5082
	323	450	0.1713	0.0003	278.010	285.7143	2.4022	1.0000	3.9237	115.95	0.5121
	323	500	0.0985	0.0017	311.169	312.5000	0.3657	1.0000	4.3006	131.35	0.4957
	323	600	0.2558	0.0027	376.802	384.6154	0.2285	1.0000	5.1985	159.15	0.4945
	323	800	0.1783	0.0015	510.591	500.0000	0.2858	1.0000	7.0496	215.56	0.4951
	323	1000	0.2558	0.0008	642.812	625.0000	0.4297	1.0000	8.8707	270.96	0.4956

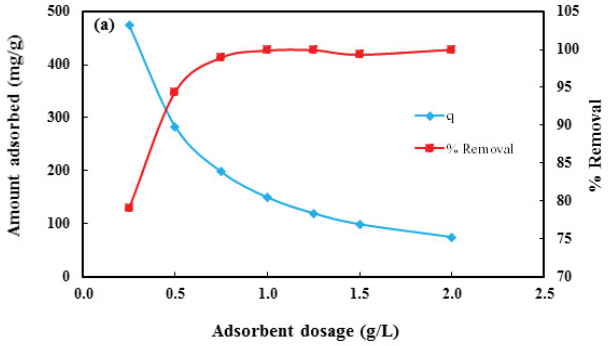

Fig. 6. Effect of clay amount on the adsorption capacity and % removal of CTAB at the adsorption time of 30 min (stirring speed = 150 min^{-1}; [CTAB]$_0$: 150 mg/L; temperature: 293 K; natural pH).

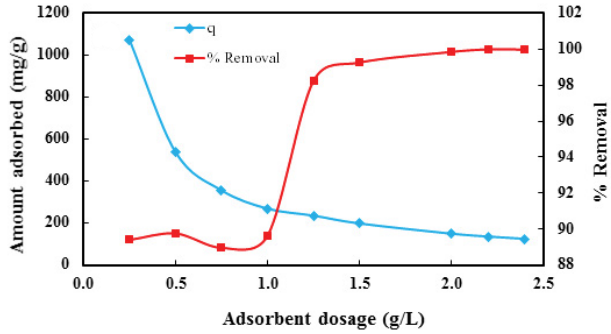

Fig. 7. Effect of clay amount on the adsorption capacity and % removal of and TTAB at the adsorption time of 30 min (stirring speed = 150 min^{-1}; [TTAB]$_0$: 300 mg/L; temperature: 293 K; natural pH).

conductivity values can be attributed to the presence of increased ionic species due to deprotonation.

3.7. Micellization studies

Micellar adsorption experiments with both CTAB and TTAB were performed at a constant stirring speed of 150 rpm, temperatures of 293, 313 and 323 K, natural pH, solid/liquid ratios of 0.8 g/L for CTAB and 1.50 g/L for TTAB. Initial concentrations for CTAB and TTAB, which are above the critical micelle concentrations of both surfactants, were chosen as 330–410 mg/L and 1,110–1,200 mg/L, respectively. The results obtained are plotted in Figs. 12 and 13, respectively, for CTAB and TTAB. From these figures, it was found that the equilibrium time for both surfactants to reach adsorption equilibrium was approximately 10 min, indicating that rapid adsorption occurred. The observed increase in adsorption capacity at saturation with increasing concentration can be attributed to the transition of micellization from spherical to ellipsoidal aggregation due to more intense van der Waals interactions between the long hydrophobic chains as a result of increased ionic strength and thus more tightly packed aggregates.

However, the graph obtained for TTAB shows that with increasing initial concentration, their adsorption

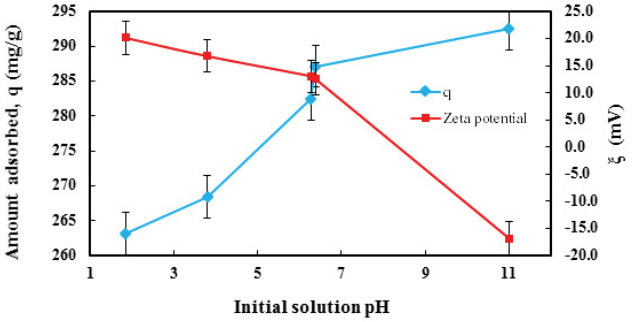

Fig. 8. Variation of zeta potential and adsorption capacity as a function of initial solution pH (temperature: 293 K; [CTAB]$_0$: 300 mg/L; [MMT]$_0$: 1.0 g/L; time: 30 min; stirring speed:150 min^{-1}).

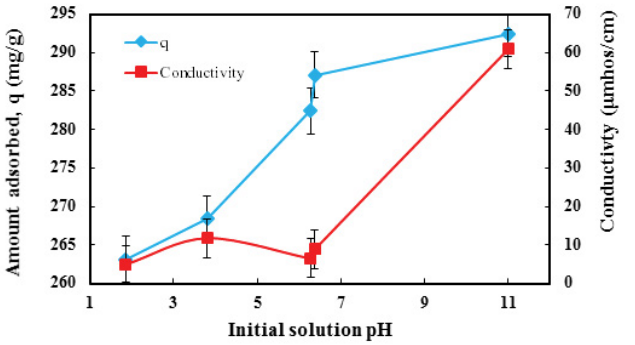

Fig. 9. Variation of conductivity and adsorption capacity as a function of initial solution pH (temperature: 293 K; [CTAB]$_0$: 300 mg/L; [MMT]$_0$: 1 g/L; time: 30 min; stirring speed: 150 min^{-1}).

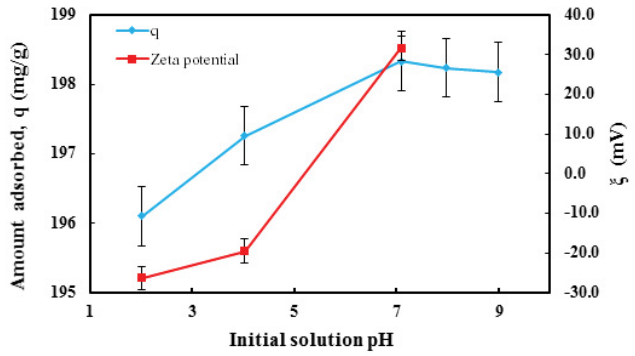

Fig. 10. Variation of zeta potential and adsorption capacity as a function of initial solution pH (temperature: 293 K; [TTAB]$_0$: 300 mg/L; [MMT]$_0$: 1.5 g/L; time: 30 min; stirring speed: 150 min^{-1}).

capacity at saturation does not increase as much as that of CTAB, indicating the decisive role of the conformation and length of the hydrophobic tail. The results obtained from the experiments carried out for 30 min at natural pH and 150 min^{-1} mixing speed to obtain the micellar adsorption isotherms of CTAB and TTAB for three temperatures, 293, 313 and 323 K, are graphed in Figs. 14 and 15.

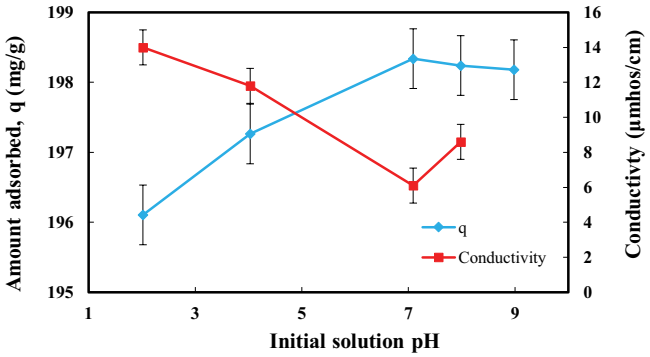

Fig. 11. Variation of conductivity and adsorption capacity as a function of initial solution pH (temperature: 293 K; $[TTAB]_0$: 300 mg/L; $[MMT]_0$: 1.5 g/L; time: 30 min; stirring speed: 150 min^{-1}).

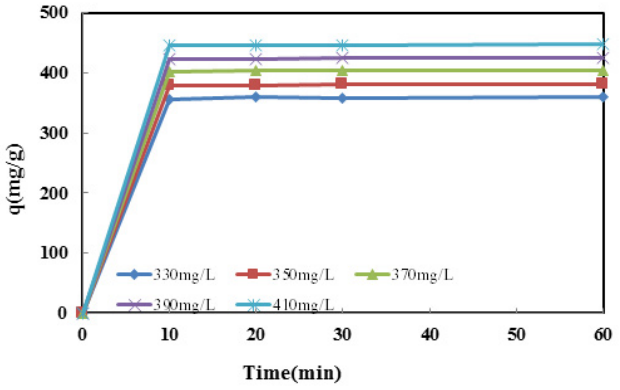

Fig. 12. Variation of the amount adsorbed (q) with adsorption time at various initial CTAB concentrations for 293 K (stirring speed: 150 min^{-1}; $[MMT]_0$: 0.8 g/L; temperature: 293 K; natural pH).

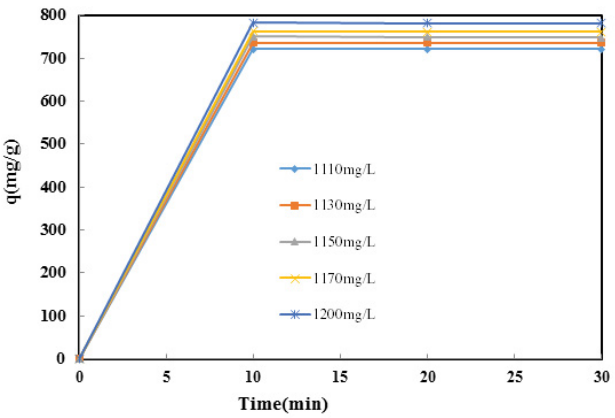

Fig. 13. Variation of the amount adsorbed (q) with adsorption time at various initial TTAB concentrations for 293 K (stirring speed: 150 min^{-1}; $[MMT]_0$: 1.5 g/L; temperature: 293 K; natural pH).

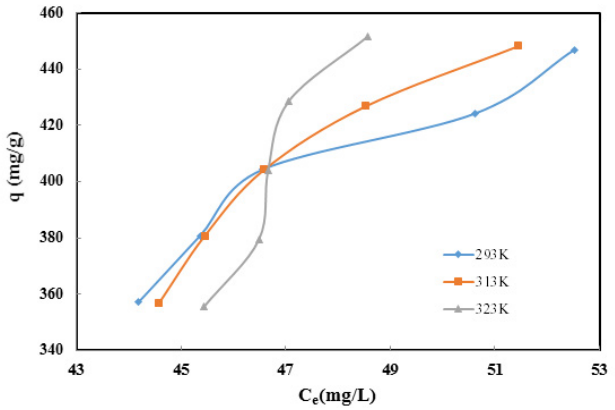

Fig. 14. Adsorption isotherms of the adsorption of CTAB on the clay at different temperatures ($[MMT]_0$: 0.8 g/L; time: 30 min; stirring speed: 150 min^{-1}; natural pH).

From Fig. 14, it is seen that the adsorbed amounts for CTAB decrease with increasing temperature up to medium equilibrium concentrations, reflecting an exothermic process nature, and then, on the contrary, exhibit an endothermic character with adsorbed values increasing with increasing temperature. At a certain point, which can be defined as an inflection or a nodal point, the isotherms coincide. For this point, it can be argued that the interaction between the chains in adsorption depending on temperature is not affected by thermal mobility, and CTAB aggregation and thus micellar adsorption are not kinetic controlled. After this point, it can be said that due to the increase in thermal mobility with increasing temperature, the hydrophobic interactions increase as the chains get closer to each other, and thus the adsorbed amounts increase due to the formation of elliptical micellar structures with lower solubility and smaller surface area. It can also be considered that the increase in thermal mobility with increasing temperature at equilibrium concentrations before the inflection point weakens the hydrophobic interactions between the chains, and thus the tendency of surfactant ions to escape from the interface surface to the bulk phase due to the repulsion between the head groups. At 293 K, that is, below the Kraft temperature of CTAB, and at low equilibrium concentrations, it is assumed that the spherical form is dominant in micelle aggregation. The appeared partial reduction in adsorption efficiency at low CTAB concentrations above the Kraft temperature of 323 K can be attributed to the increased spherical aggregation stability due to the high temperature. The observed partial increase in adsorption efficiency at high CTAB concentrations can be associated the increase in ellipsoid aggregation tendency owing to the high concentration.

As can be seen from the micellar adsorption isotherm curves of TTAB in Fig. 15, the adsorbed amounts generally tend to decrease with increasing temperature, but irregular changes in isotherm shapes occur at all temperatures. As it is known, decreasing chain length reduces the aggregation tendency of hydrophobic tails, and increasing temperature can both increase thermal mobility and control the hydrophobic interaction energy, which can lead to chain separation and

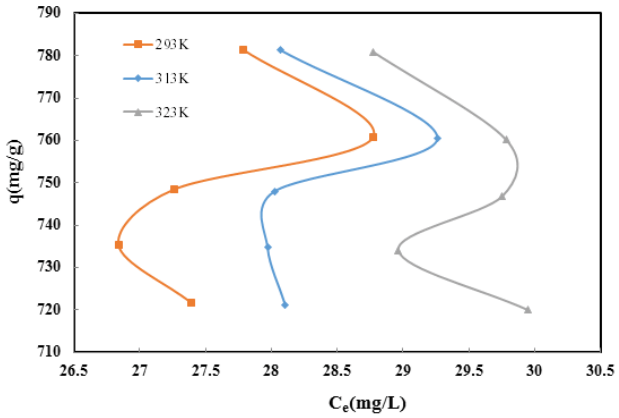

Fig. 15. Adsorption isotherms of the adsorption of TTAB on the clay at different temperatures ([MMT]$_0$: 1.5 g/L; time: 30 min; stirring speed: 150 min^{-1}; natural pH).

increased solubility, as well as an increase in the degree of counter-ion dissociation. Exothermic adsorption enthalpy shows the major role of London dispersion forces in micelle formation [41]. Due to the fact that adsorption takes place with micelles, competing aggregation-deaggregation tendencies depending on temperature and tail length can be considered as the cause of irregularity in isotherm shapes.

In order to evaluate the changes in the surface morphology of clay particles after micelle adsorption of both surfactants, the SEM images of the samples obtained from the adsorption experiments made at a solid/liquid ratio of 1.0 g/L and at different initial surfactant concentrations (300, 330 and 410 mg/L for CTAB and 1,090, 1,130 and 1,150 mg/L for TTAB) were taken. The images for CTAB and TTAB are shown in Figs. 16 and 17, respectively.

It can be seen from Fig. 16 that the raw MMT exhibits heterogeneous surface morphology with prominent fractures and phase separations. Again, this figure may shows that after CTAB adsorption at various concentrations above the critical micelle concentration (CMC), the clay particles interact more closely with each other, thus resulting in a more homogeneous compact surface morphology with increasing concentration. It can be seen from Fig. 17 that after adsorption of TTAB at various concentrations above the critical micelle concentration (CMC), a surface morphology emerges indicating that the interactions of the clay particles with each other are weaker than in the CTAB adsorbed samples, and they aggregate in a way that reflects the raw clay structure.

In order to compare the results of CTAB and TTAB adsorption with those obtained from some previous studies, the findings are presented in Table 5 considering the adsorbent, adsorbate, adsorption type and adsorbed amount, as well as the monomeric and micellar adsorption performances of CTAB and TTAB.

From this table it can be seen that monomeric and micellar adsorption of CTAB and TTAB on clay can occur at sufficiently high ratio in a relatively short time.

4. Conclusion

The monomeric and micellar adsorption of cationic surfactants with two different chain lengths such as CTAB and TTAB on the clay surface were investigated comparatively. For this, various parameters such as adsorption time, initial surfactant concentration, temperature, clay dosage and initial solution pH were chosen. The results were supported by conductivity measurements and the zeta potential of the particles. It has been concluded that a short time such as 5 min is sufficient to reach equilibrium adsorption, and therefore adsorption occurs predominantly through physical interactions. From the obtained adsorption isotherms, it can be argued that ion exchange mechanism is effective at low surfactant concentrations, and ion pairing and hydrophobic bonding mechanisms are effective at higher concentrations. Thermodynamic data revealed that the adsorption was physical and exothermic in character and was spontaneous. Adsorption enthalpy and entropy changes for both adsorbates were calculated as –10.6 and –6.6 kJ/mol and 18.0 and 14.9 J/mol K, respectively. In addition, the adsorption data were applied to various adsorption isotherm models and the order of fit was obtained as

Table 5
Comparison of monomeric and micellar adsorption performances of CTAB and TTAB with the results of some previous studies

Adsorbent	Adsorbate	Adsorption type	Adsorbed amount	References
Silica/silicon surface	CTAB	Micelle	3.6 mmol/m^2	[42]
Clay	CTAB	Monomer Micelle	125.78 mg/g ≈180 mg/g	[13]
Coals	CTAB	Monomer	1.26–1.54 mmol/g	[43]
Montmorillonite	CTAB	Monomer	14.84 mg/g-Mt	[44]
TH90 activated carbon	C16TABr C14TABr	Monomer	0.85 ± 0.01 mmol/g 0.80 ± 0.01 mmol/g	[39]
Lignite	DTAB	Monomer	≈0.15 mmol/g	[45]
Bituminous coal Clay	CTAB	Monomer	0.65 mmol/g 3.24 mmol/g	[46]
Clay	CTAB TTAB	Monomer	312.5 mg/g 285.71 mg/g	This study

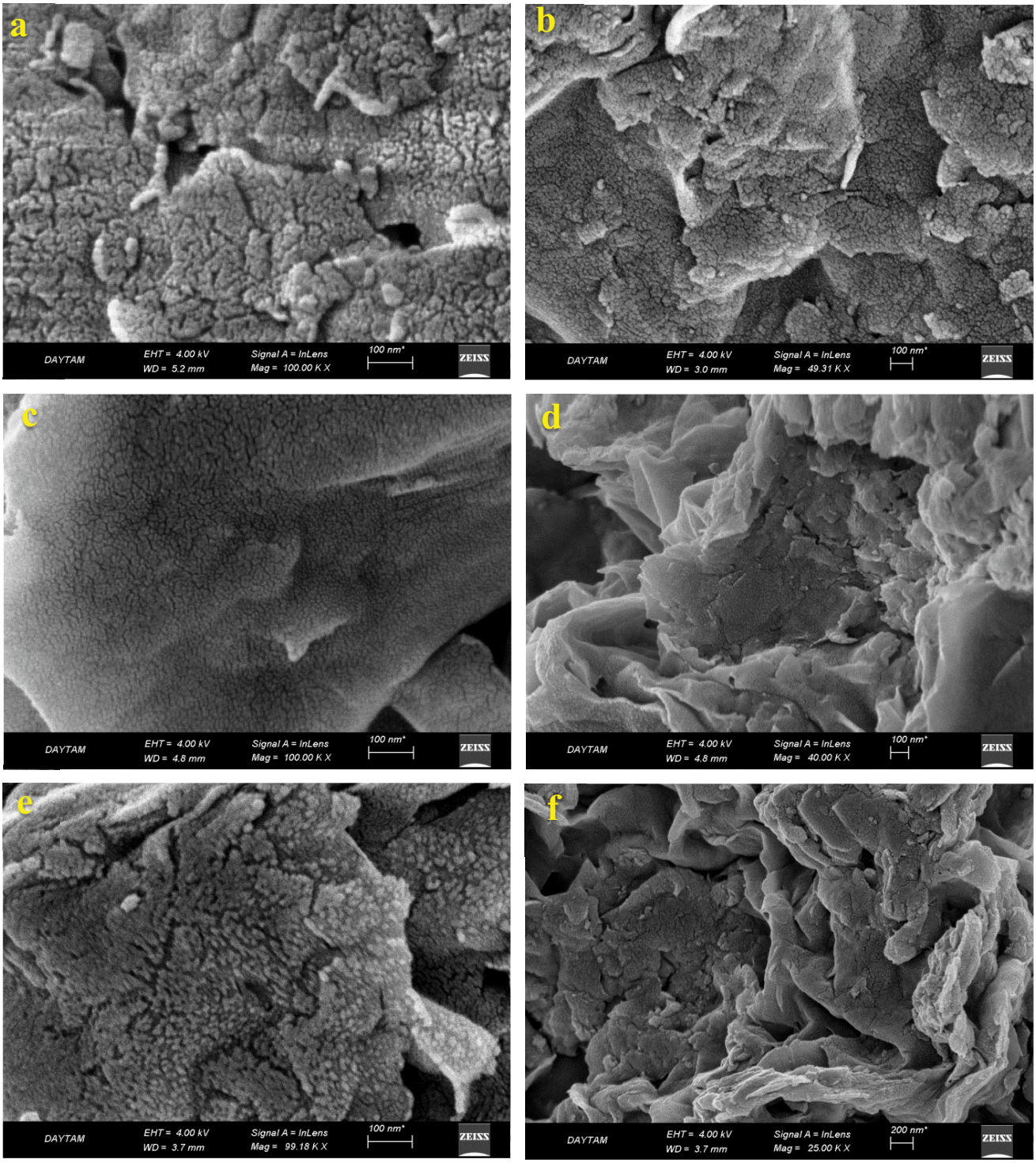

Fig. 16. SEM images of (a) raw Mt, (b) CTAB/Mt (300 mg/L), (c,d) CTAB/Mt (330 mg/L), and (e,f) CTAB/Mt (410 mg/L).

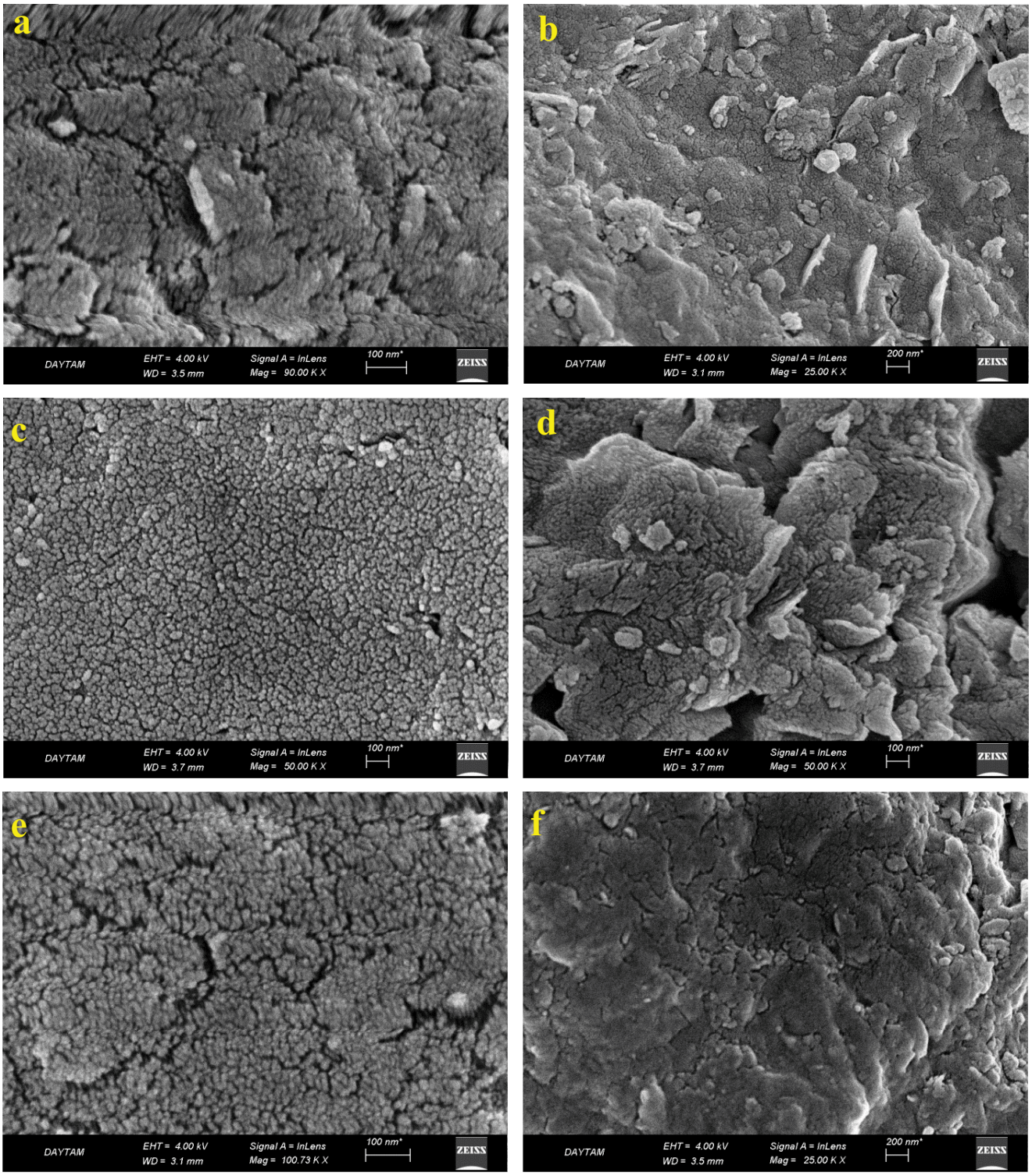

Fig. 17. SEM images of (a,b) TTAB/Mt (1,090 mg/L), (c,d) TTAB/Mt (1,130 mg/L), and (e,f) TTAB/Mt (1,150 mg/L).

Langmuir > Freundlich > Temkin > Dubinin–Radushkevich for CTAB and as Langmuir > Temkin > Freundlich > Dubi nin–Radushkevich for TTAB. The monolayer adsorption capacities for both adsorbates were found to be 312.50 and 285.71 mg/g, respectively. Kinetic studies have shown that the rate of adsorption can be more representative of the pseudo-second-order model for both surfactants, which implies the presence of strong physical interactions between clay particles and surfactant ions. micellar adsorption studies performed at concentrations above the critical micelle concentration (CMC) for both surfactants revealed that the change in the formed micelle forms with the increase in temperature and initial surfactant concentration for both surfactants was also reflected in their adsorption behavior. The different behaviors of CTAB and TTAB were associated with the difference in their hydrophobic tail lengths, and from the obtained SEM images, it was concluded that especially the micellar adsorption of CTAB indicates more intense interaction and thus tighter stacking.

Declaration of competing interest

The authors declare that they have no known competing financial interests or personal relationships that could have appeared to influence the work reported in this paper.

Acknowledgments

The authors would like to thank Atatürk University for its financial support (Project No: 2012/153) and the East Anatolia High Technology Application and Research Center (DAYTAM) for technical support.

References

[1] L. Guerrero-Hernández, H.I. Meléndez-Ortiz, G.Y. Cortez-Mazatan, S. Vaillant-Sánchez, R.D. Peralta-Rodríguez, Gemini and bicephalous surfactants: a review on their synthesis, micelle formation, and uses, Int. J. Mol. Sci., 23 (2022) 1798, doi: 10.3390/ijms23031798.
[2] N.-M. Lee, B.-H. Lee, Thermodynamics on the micellization of various pure and mixed surfactants: effects of head- and tail-groups, J. Chem. Thermodyn., 95 (2016) 15–20.
[3] X. Cui, Y. Jiang, C. Yang, X. Lu, H. Chen, S. Mao, M. Liu, H. Yuan, P. Luo, Y. Du, Mechanism of the mixed surfactant micelle formation, J. Phys. Chem. B, 114 (2010) 7808–7816.
[4] E. Brodskaya, Role of water in the formation of the electric double layer of micelles, J. Phys. Chem., B, 116 (2012) 5795–5800.
[5] H.I. Tantry, F.A. Sheikh, P.A. Bhat, Micellization behavior of dodecylethyldimethylammonium bromide as a function of temperature and concentration, J. Mol. Liq., 183 (2013) 79–84.
[6] N. Lourith, M. Kanlayavattanakul, Natural surfactants used in cosmetics: glycolipids, Int. J. Cosmet. Sci., 31 (2009) 255–261.
[7] P.K. Sen, P. Chatterjee, B. Pal, Evidence of co-operativity in the pre-micellar region in the hydrolytic cleavage of phenyl salicylate in the presence of cationic surfactants of CTAB, TTAB and CPC, J. Mol. Catal. A: Chem., 396 (2015) 23–30.
[8] M. Guin, R.A. Roopa, P. Jain, N.B. Singh, Heterocyclic surfactants and their applications in cosmetics, ChemistrySelect, 7 (2022) e202103989, doi: 10.1002/slct.202103989.
[9] S.M. Shaban, A.S. Fouda, M.A. Elmorsi, T. Fayed, O. Azazy, Adsorption and micellization behavior of synthesized amidoamine cationic surfactants and their biological activity, J. Mol. Liq., 216 (2016) 284–292.
[10] A. Zdziennicka, K. Szymczyk, J. Krawczyk, B. Janczuk, Critical micelle concentration of some surfactants and thermodynamic parameters of their micellization, Fluid Phase Equilib., 322 (2012) 126–134.
[11] N. Pal, M. Vajpayee, A. Mandal, Cationic/nonionic mixed surfactants as enhanced oil recovery fluids: influence of mixed micellization and polymer association on interfacial, rheological, and rock-wetting characteristics, Energy Fuels, 33 (2019) 6048–6059.
[12] R. Zhang, P. Somasundaran, Advances in adsorption of surfactants and their mixtures at solid/solution interfaces, Adv. Colloid Interface Sci., 123–126 (2006) 213–229.
[13] A. Gürses, S. Karaca, F. Aksakal, M. Açikyildiz, Monomer and micellar adsorptions of CTAB onto the clay/water interface, Desalination, 264 (2010) 165–172.
[14] G.F. Wang, S. Wang, Z.M. Sun, S.L. Zheng, Y.F. Xi, Structures of nonionic surfactant modified montmorillonites and their enhanced adsorption capacities towards a cationic organic dye, Appl. Clay Sci., 148 (2017) 1–10.
[15] A.M. Awad, S.M.R. Shaikh, R. Jalab, M.H. Gulied, M.S. Nasser, A. Benamor, S. Adham, Adsorption of organic pollutants by natural and modified clays: a comprehensive review, Sep. Purif. Technol., 228 (2019) 115719, doi: 10.1016/j.seppur.2019.115719.
[16] Ö. Açışlı, S. Karaca, A. Gürses, Investigation of the alkyl chain lengths of surfactants on their adsorption by montmorillonite (Mt) from aqueous solutions, Appl. Clay Sci., 142 (2017) 90–99.
[17] J. Chanra, E. Budianto, B. Soegijono, Surface modification of montmorillonite by the use of organic cations via conventional ion exchange method, IOP Conf. Ser.: Mater. Sci. Eng., 509 (2019) 012057.
[18] P.T. Hang, G. Brindley, Methylene blue absorption by clay minerals. Determination of surface areas and cation exchange capacities (clay-organic studies XVIII), Clay Clay Miner., 18 (1970) 203–212.
[19] A. Gurses, A. Hassani, M. Kiransan, O. Acisli, S. Karaca, Removal of methylene blue from aqueous solution using by untreated lignite as potential low-cost adsorbent: kinetic, thermodynamic and equilibrium approach, J. Water Process Eng., 2 (2014) 10–21.
[20] P.S. Ghosal, A.K. Gupta, Determination of thermodynamic parameters from Langmuir isotherm constant-revisited, J. Mol. Liq., 225 (2017) 137–146.
[21] E.C. Lima, A. Hosseini-Bandegharaei, J.C. Moreno-Pirajan, I. Anastopoulos, A critical review of the estimation of the thermodynamic parameters on adsorption equilibria. Wrong use of equilibrium constant in the Van't Hoof equation for calculation of thermodynamic parameters of adsorption, J. Mol. Liq., 273 (2019) 425–434.
[22] P. Saha, S. Datta, Assessment on thermodynamics and kinetics parameters on reduction of methylene blue dye using flyash, Desal. Water Treat., 12 (2009) 219–228.
[23] P. Saha, Assessment on the removal of Methylene blue dye using tamarind fruit shell as biosorbent, Water, Air, Soil Pollut., 213 (2010) 287–299.
[24] A. Hassani, A. Khataee, S. Karaca, Photocatalytic degradation of ciprofloxacin by synthesized TiO_2 nanoparticles on montmorillonite: effect of operation parameters and artificial neural network modeling, J. Mol. Catal. A: Chem., 409 (2015) 149–161.
[25] I. El Younssi, T. Rhadfi, A. Atlamsani, J.-P. Quisefit, F. Herbst, K. Draoui, K-10 montmorillonite: an efficient and reusable catalyst for the aerobic CC bond cleavage of α-substituted ketones, J. Mol. Catal. A: Chem., 363–364 (2012) 437–445.
[26] F. Rasouli, S. Aber, D. Salari, A.R. Khataee, Optimized removal of Reactive Navy Blue SP-BR by organo-montmorillonite based adsorbents through central composite design, Appl. Clay Sci., 87 (2014) 228–234.
[27] S. Chowdhury, S. Chakraborty, P. Saha, Biosorption of Basic Green 4 from aqueous solution by *Ananas comosus* (pineapple) leaf powder, Colloids Surf., B, 84 (2011) 520–527.
[28] C. Muthukumaran, V.M. Sivakumar, M. Thirumarimurugan, Adsorption isotherms and kinetic studies of crystal violet dye

removal from aqueous solution using surfactant modified magnetic nanoadsorbent, J. Taiwan Inst. Chem. Eng., 63 (2016) 354–362.
[29] M. Sharma, S. Hazra, S. Basu, Kinetic and isotherm studies on adsorption of toxic pollutants using porous ZnO@SiO_2 monolith, J. Colloid Interface Sci., 504 (2017) 669–679.
[30] K. Wattanakul, H. Manuspiya, N. Yanumet, The adsorption of cationic surfactants on BN surface: its effects on the thermal conductivity and mechanical properties of BN-epoxy composite, Colloids Surf., A, 369 (2010) 203–210.
[31] A. Gürses, K. Güneş, F. Mindivan, M.E. Korucu, M. Açıkyıldız, Ç. Doğar, The investigation of electrokinetic behaviour of micro-particles produced by CTA+ ions and Na-montmorillonite, Appl. Surf. Sci., 318 (2014) 79–84.
[32] A. Bera, T. Kumar, K. Ojha, A. Mandal, Adsorption of surfactants on sand surface in enhanced oil recovery: isotherms, kinetics and thermodynamic studies, Appl. Surf. Sci., 284 (2013) 87–99.
[33] A.R. Bagheri, M. Ghaedi, A. Asfaram, A.A. Bazrafshan, R. Jannesar, Comparative study on ultrasonic assisted adsorption of dyes from single system onto Fe_3O_4 magnetite nanoparticles loaded on activated carbon: experimental design methodology, Ultrason. Sonochem., 34 (2017) 294–304.
[34] K.Y. Foo, B.H. Hameed, Insights into the modeling of adsorption isotherm systems, Chem. Eng. J., 156 (2010) 2–10.
[35] S. Chowdhury, P.D. Saha, Biosorption kinetics, thermodynamics and isosteric heat of sorption of Cu(II) onto *Tamarindus indica* seed powder, Colloids Surf., B, 88 (2011) 697–705.
[36] B. Hameed, D. Mahmoud, A. Ahmad, Equilibrium modeling and kinetic studies on the adsorption of basic dye by a low-cost adsorbent: coconut (*Cocos nucifera*) bunch waste, J. Hazard. Mater., 158 (2008) 65–72.
[37] M. Temkin, V. Pyzhev, Recent modifications to Langmuir isotherms, Acta Physiochim, URSS, 12 (1940) 217–222.
[38] L. Zhou, J. Jin, Z. Liu, X. Liang, C. Shang, Adsorption of acid dyes from aqueous solutions by the ethylenediamine-modified magnetic chitosan nanoparticles, J. Hazard. Mater., 185 (2011) 1045–1052.
[39] M.G. Krivova, D.D. Grinshpan, N. Hedin, Adsorption of CnTABr surfactants on activated carbons, Colloids Surf., A, 436 (2013) 62–70.
[40] K.A. Tan, N. Morad, T.T. Teng, I. Norli, Synthesis of magnetic nanocomposites (AMMC-Fe_3O_4) for cationic dye removal: optimization, kinetic, isotherm, and thermodynamics analysis, J. Taiwan Inst. Chem. Eng., 54 (2015) 96–108.
[41] A. Pal, S. Chaudhary, Thermodynamic and aggregation behavior of aqueous tetradecyltrimethylammonium bromide in the presence of the hydrophobic ionic liquid 3-methyl-1-pentylimidazolium hexafluorophosphate, J. Mol. Liq., 207 (2015) 67–72.
[42] V.K. Paruchuri, K.Q. Fa, B.M. Moudgil, J.D. Miller, Adsorption density of spherical cetyltrimethylammonium bromide (CTAB) micelles at a silica/silicon surface, Appl. Spectrosc., 59 (2005) 668–672.
[43] R. Marsalek, J. Pospisil, B. Taraba, The influence of temperature on the adsorption of CTAB on coals, Colloids Surf., A, 383 (2011) 80–85.
[44] A. Moslemizadeh, S.K.Y. Aghdam, K. Shahbazi, H.K.Y. Aghdam, F. Alboghobeish, Assessment of swelling inhibitive effect of CTAB adsorption on montmorillonite in aqueous phase, Appl. Clay Sci., 127 (2016) 111–122.
[45] J. Guo, Y. Xia, Y. Liu, S. Liu, L. Zhang, B. Li, Microscopic adsorption behaviors of ionic surfactants on lignite surface and its effect on the wettability of lignite: a simulation and experimental study, J. Mol. Liq., 345 (2022) 117851, doi: 10.1016/j.molliq.2021.117851.
[46] R. Maršálek, Z. Navrátilová, Comparative study of CTAB adsorption on bituminous coal and clay mineral, Chem. Pap., 65 (2011) 77–84.